

## Deep Learning Module for Spectroscopic Identification of Pathogenic Bacteria

Manish Surjuse<sup>1</sup>, Vijaya Yaduvanshi<sup>2</sup>, Abhijeet Lonkar<sup>3</sup>, Siddharth Mathane<sup>4</sup>

E&TC Department, SKNCOE, SPPU, Pune, India

[1manishsurjuse581@gmail.com](mailto:manishsurjuse581@gmail.com)

[2vijaya.yaduvanshi\\_skncoe@sinhgad.edu](mailto:vijaya.yaduvanshi_skncoe@sinhgad.edu)

[3abhijeetlonkar123@gmail.com](mailto:abhijeetlonkar123@gmail.com)

[4siddharthmathane10@gmail.com](mailto:siddharthmathane10@gmail.com)

**Abstract**— Bacterial infections are a major threat to the health-care sector and a leading cause of death in many countries. According to the study, over 15 million antibiotic-resistant infections occur in the India each year, resulting in over 170,000 deaths. To overcome the problem an intelligent techniques like computer vision in a single stage, it promises label-free bacterial detection, recognition, and antibiotic susceptibility testing. Traditional sample clustering is the latest diagnostic approach which is used to detect and identify the bacteria and its antibiotic susceptibility. This procedure is leisure process and it takes around seven days even in acknowledged laboratories. This led to wide range of generic antibiotics in prescription while patient is still waiting for the result. Utilization of antibiotics may cause side effects such as anti-microbial resistance, drug infections, digestive problems, fungal infections. Intelligent technique for rapid, culture free diagnosis of bacterial infection is enabling earlier prescription of target antibiotics and helps mitigate antimicrobial resistance.

**Keywords**— Clustering, Pathogens, Diagnosis, Antibiotic, Computer Vision

### I. INTRODUCTION

Bacterial infections are one of the biggest threats to the health industry and a leading cause of death across the nations, claiming more than 6.7 million lives each year. According to the report, more than 15 million antibiotic-resistant infections occur in the U.S. each year, and more than 170,000 people die as a result. In addition, 223,900 cases of *Chloridoids difficile* occurred in 2017 and at least 12,800 people died. To overcome this problem, we are with the intelligent technique for medical diagnosis of pathogens. The live scenario for medical diagnosis is the traditional method in which lab testing in which they collect samples and test it. This process is slow and it takes 5-7 days. This led to wide range of generic antibiotics in prescription that cause side effect while patient is still waiting for the result. The other method is Spectroscopic methods like Raman Spectroscopy combined with Computer Vision techniques which is mainly Convolutional Neural Networks and Artificial Neural Networks architecture is a new way of culture free diagnosis. Additionally, spectroscopy like confocal spectroscopy can be used to recognize individual bacterial cells. Different bacterial phenotypes have different chemical compositions, which results in tiny changes in their Raman spectra. Due to the low effectiveness of Raman scattering, these tiny spectrum variations are easily detected by background noise. To achieve high identification accuracies, a high signal to noise ratio is required. An additional problem is the demand for complete datasets that are not collected in research for species differentiation. Because of the scarcity of data, there is a large bias towards the training set, which makes predictions difficult. This issue can be solved by

adding more spectroscopic data to our data set to create variance, and then utilizing regularization approaches when training.

## II. LITERATURE SURVEY

Resnet: Generalizing Residual Architectures [8]. On difficult computer vision tasks, residual networks (Res Nets) have recently achieved state-of-the-art status. They implement Resnet in Resnet (RiR), generalized deep dual-stream architecture. It is simple to implement and has no computational overhead when using Res Nets and regular CNNs. RiR outperforms Res Nets on CIFAR-10 and creates a new state-of-the-art on CIFAR-100, outperforming architectures with comparable quantities of augmentation. It's more difficult to train deeper neural networks. We present a residual learning system for training networks that are much deeper than previously used networks. Instead of learning unreferenced functions, we directly reformulate the layers as learning residual functions with relation to the layer inputs. We present extensive empirical evidence demonstrating that residual networks are simpler to optimize and can gain accuracy from significantly increased depth.

Raman Spectroscopies in the detection of hazardous material. Baltic URSI Symposium (URSI) [13]. In this paper explain a Raman spectroscopy has become a common technique for first responders to identify hazardous materials. However, considering its many benefits, this strategy has a drawback: it has a low sensitivity. Surfaced Enhanced Raman Spectroscopy, a technique that has yet to see real-world applications, could solve this constraint. They offer a summary of approaches, Raman spectroscopies, and examples of how they've been used to detect and identify biological, chemical, and explosive materials in this paper. Spectroscopic techniques, such as Raman spectroscopy, which is based on inelastic light scattering, meet this requirement. This method, on the other hand, is designed to identify vast quantities of materials.

Perceptron-based learning algorithms. IEEE Transactions on Neural Networks [5] in this paper, the creation and study of learning algorithms is a crucial activity for connectionist science. Several supervised learning algorithms for single-cell and network models are investigated. The pocket algorithm, a modification of perceptron learning that makes perceptron learning work well with non-separable training data, even if the data is noisy and contradictory, is at the heart of these algorithms. These algorithms have the following characteristics: speed algorithms that can manage large sets of training data; network scaling properties, i.e., network methods scale up just as well as single-cell models when the number of inputs is increased; analytic tractability, i.e., upper bounds on classification error can be deduced; and analytic tractability, i.e., upper bounds on classification error can be deduced. online education.

## III. PROPOSED DESIGN

The block diagram fig (1) will show the implementation of the model using traditional method and computer vision method using deep learning.

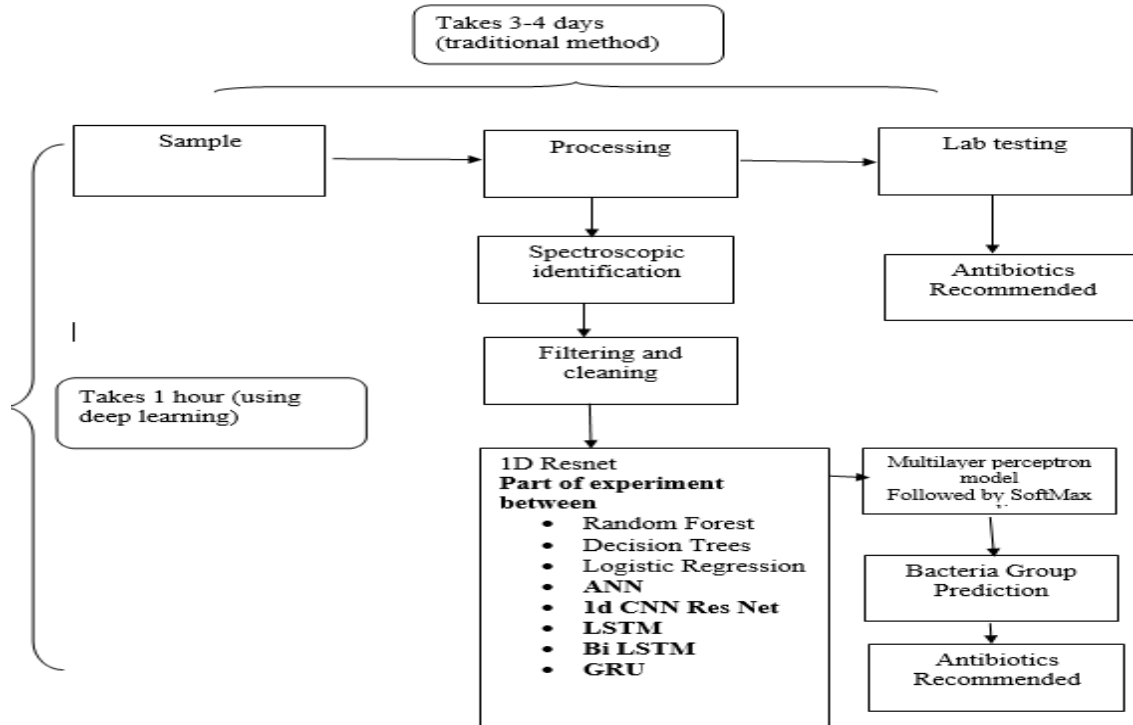


Fig. 1 Model for bacteria detection

*Block Diagram Description*

**Processing** → Lab processing of the sample.

**Lab Testing** → Traditional diagnostic methods which takes ~ 7 days even in the state-of-the-art hospitals.

**Spectroscopic identification** → Creating Raman spectra through Spectro photometer.

**Filtering and cleaning** → the input for maximum feature extraction.

**1D Resnet** → Extracts trends and spatial features.

**MLP** → Based on the features extracted, this is a decision-making ANN network.

**Group Prediction** → Predicting the group of bacterial, a group represents all the bacterial which can be treated with similar anti biotics.

As far the prediction of the model the antibiotics is suggested in 1 hour including testing procedures.

IV. IMPLEMENTATION

*Deep Neural Network*

Neural networks are made up of layers of computational units (neurons) linked by links between them. These networks change data – such as pixels in an image or words in a text – before they can identify it as an output, such as naming an object in an image or, in our case, spectroscopic data classification.

Each neuron in a network transforms data by performing a series of calculations: a neuron multiplies an initial value by a weight, adds the result to other values coming into the same neuron, changes the result by the neuron's bias, and then normalizes the performance with an activation feature. The bias is a neuron-specific number that changes the neuron's value after all connections have been processed, and the activation mechanism ensures that values passed on are within a tunable, predicted range. This process is repeated until the final output layer can provide scores or predictions for the classification task at hand, such as the probability of finding a dog in a picture.

The network accomplishes this by comparing initial outputs to a given correct response, or goal. The initial outputs are modified using a cost function based on the degree to which they vary from the target values. Finally, the effects of the cost function are applied to both neurons and connections in order to change the biases and weights. Backpropagation is the secret to how a neural network learns a specific task by using this push-back approach. If we give these neural networks enough data from different clusters, they can directly detect the differences between them and predict the cluster of unknown samples.

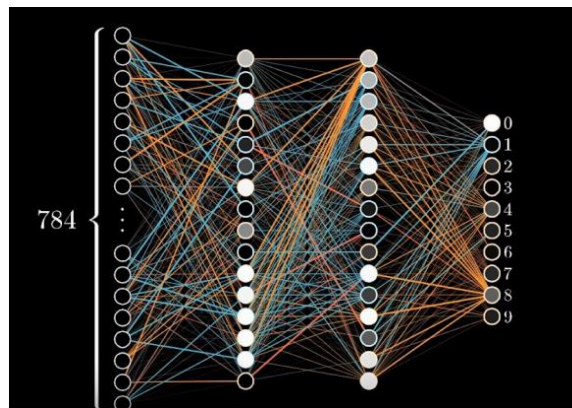


Fig. 2 An artificial neural network with 784 inputs features and 10 prediction classes

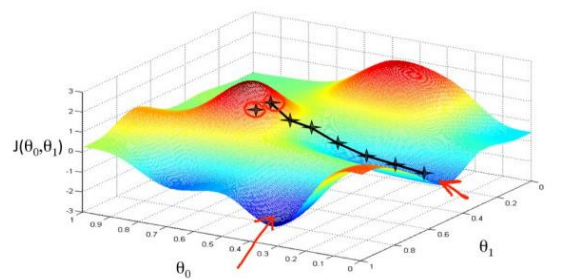


Fig. 3 The neural network optimizes itself using backpropagation algorithm to get the weight of the corresponding to the minima

*Architecture Used*

Convolutional Neural Network based Resnet architecture is being used in the work. This architecture is widely successful across a range of computer vision tasks. Structure for the neural network architecture is provided.

layer name	output size	18-layer	34-layer	50-layer	101-layer	152-layer
conv1	112×112	7×7, 64, stride 2				
		3×3 max pool, stride 2				
conv2.x	56×56	$\begin{bmatrix} 3 \times 3, 64 \\ 3 \times 3, 64 \end{bmatrix} \times 2$	$\begin{bmatrix} 3 \times 3, 64 \\ 3 \times 3, 64 \end{bmatrix} \times 3$	$\begin{bmatrix} 1 \times 1, 64 \\ 3 \times 3, 64 \\ 1 \times 1, 256 \end{bmatrix} \times 3$	$\begin{bmatrix} 1 \times 1, 64 \\ 3 \times 3, 64 \\ 1 \times 1, 256 \end{bmatrix} \times 3$	$\begin{bmatrix} 1 \times 1, 64 \\ 3 \times 3, 64 \\ 1 \times 1, 256 \end{bmatrix} \times 3$
conv3.x	28×28	$\begin{bmatrix} 3 \times 3, 128 \\ 3 \times 3, 128 \end{bmatrix} \times 2$	$\begin{bmatrix} 3 \times 3, 128 \\ 3 \times 3, 128 \end{bmatrix} \times 4$	$\begin{bmatrix} 1 \times 1, 128 \\ 3 \times 3, 128 \\ 1 \times 1, 512 \end{bmatrix} \times 4$	$\begin{bmatrix} 1 \times 1, 128 \\ 3 \times 3, 128 \\ 1 \times 1, 512 \end{bmatrix} \times 4$	$\begin{bmatrix} 1 \times 1, 128 \\ 3 \times 3, 128 \\ 1 \times 1, 512 \end{bmatrix} \times 8$
conv4.x	14×14	$\begin{bmatrix} 3 \times 3, 256 \\ 3 \times 3, 256 \end{bmatrix} \times 2$	$\begin{bmatrix} 3 \times 3, 256 \\ 3 \times 3, 256 \end{bmatrix} \times 6$	$\begin{bmatrix} 1 \times 1, 256 \\ 3 \times 3, 256 \\ 1 \times 1, 1024 \end{bmatrix} \times 6$	$\begin{bmatrix} 1 \times 1, 256 \\ 3 \times 3, 256 \\ 1 \times 1, 1024 \end{bmatrix} \times 23$	$\begin{bmatrix} 1 \times 1, 256 \\ 3 \times 3, 256 \\ 1 \times 1, 1024 \end{bmatrix} \times 36$
conv5.x	7×7	$\begin{bmatrix} 3 \times 3, 512 \\ 3 \times 3, 512 \end{bmatrix} \times 2$	$\begin{bmatrix} 3 \times 3, 512 \\ 3 \times 3, 512 \end{bmatrix} \times 3$	$\begin{bmatrix} 1 \times 1, 512 \\ 3 \times 3, 512 \\ 1 \times 1, 2048 \end{bmatrix} \times 3$	$\begin{bmatrix} 1 \times 1, 512 \\ 3 \times 3, 512 \\ 1 \times 1, 2048 \end{bmatrix} \times 3$	$\begin{bmatrix} 1 \times 1, 512 \\ 3 \times 3, 512 \\ 1 \times 1, 2048 \end{bmatrix} \times 3$
	1×1	average pool, 1000-d fc, softmax				

Fig. 4 ResNet-based architecture

On the isolate classification mission, these architecture hyperparameters were chosen through grid search using a single training and validation split. We also tried simple MLP (multi-layer perceptron) and CNN architectures, but the Resnet-based architecture proved to be the most efficient.

## V. Results

The dataset contains 1000 features X 80,000 samples dataset with 30 label classes of bacteria. This dataset is taken from Stanford Hospital in year 2016-17. These 30 classes cover 94% of all bacterial infection treated by Stanford Hospital. For testing we have 12,000 blood samples from year 2019 of class MRSA and MSSA.

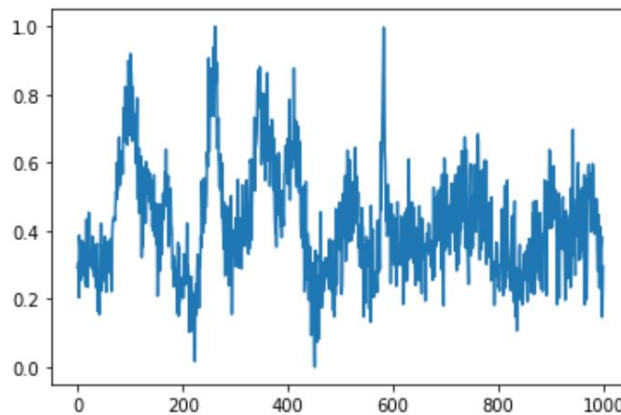


Fig. 5 The spectral representation of blood sample of *C. glabrata*

We train the neural network on a 30-class detection task, where CNN outputs a probable distribution across 30 reference class and the maximum is taken as predicted class as shown in figure 6.

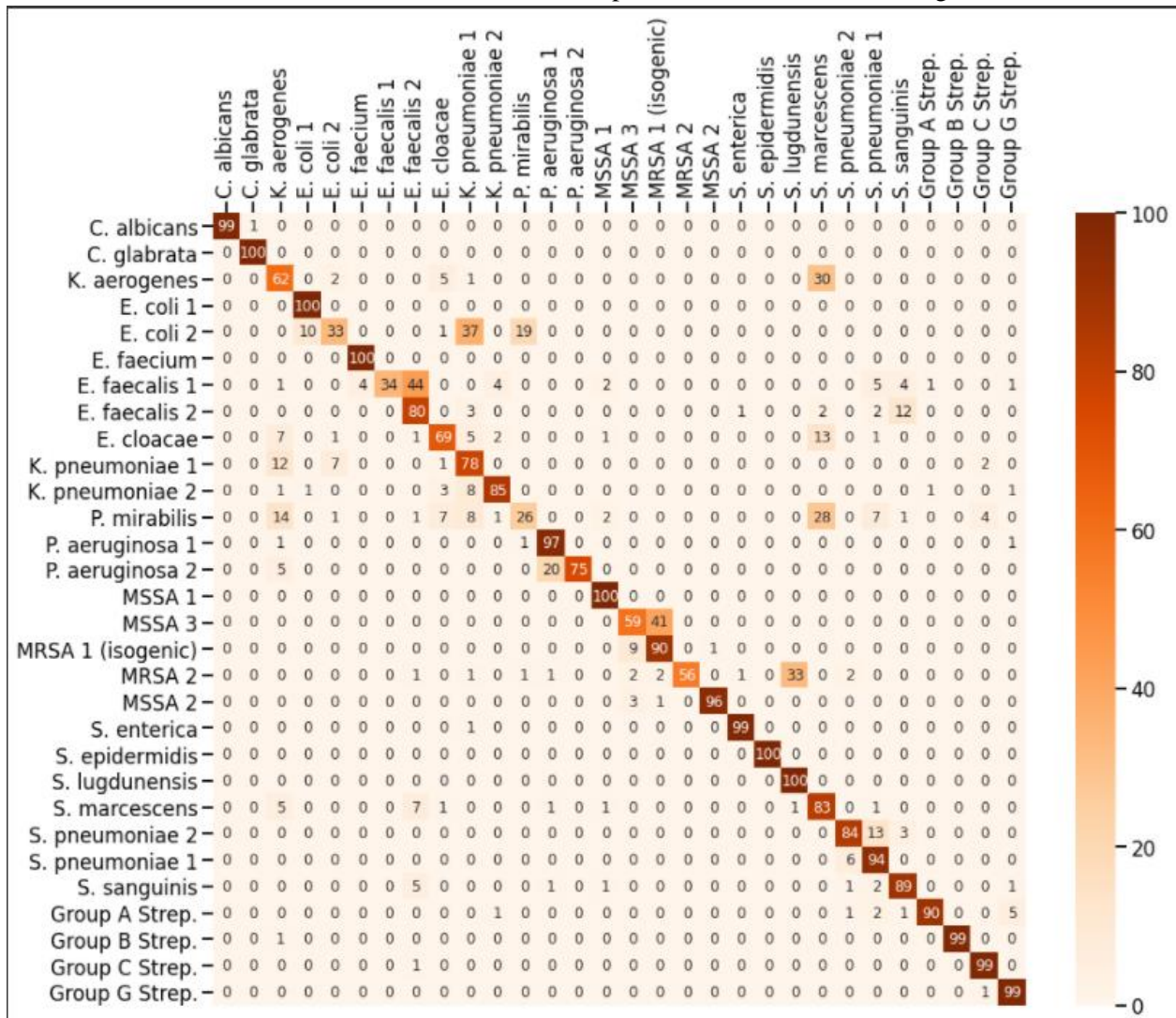


Fig. 6 Confusion matrix of 30 bacterial classes which is trained by CNN

As from Fig. 5, MSSA 1, E. coli 2, MRSA 2 this bacterial class having less than 60% predictive rate as they are similar structure to the adjacent bacterial group that result in low predictive accuracy.



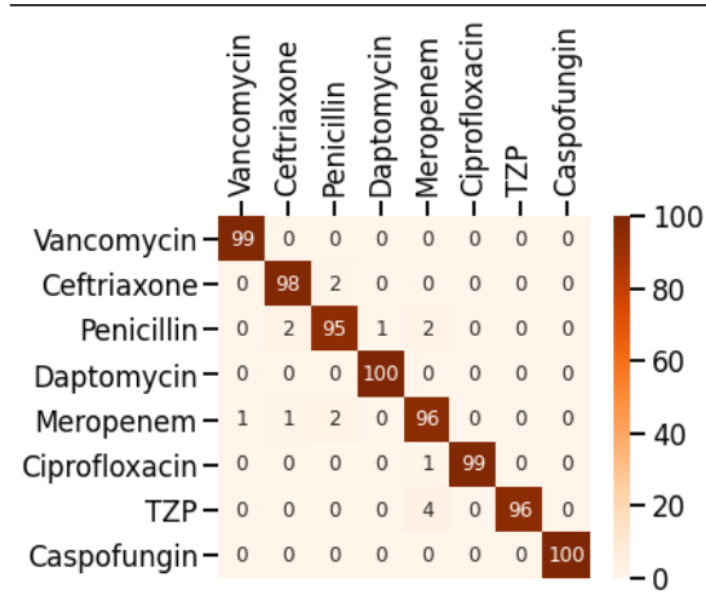


Fig. 7 The antibiotics confusion matrix

In Fig. 7, the antibiotics prediction confusion matrix is represented were the overall accuracy for predicting antibiotics is 95%, therefore the antibiotics recommendation accuracy is 95%.

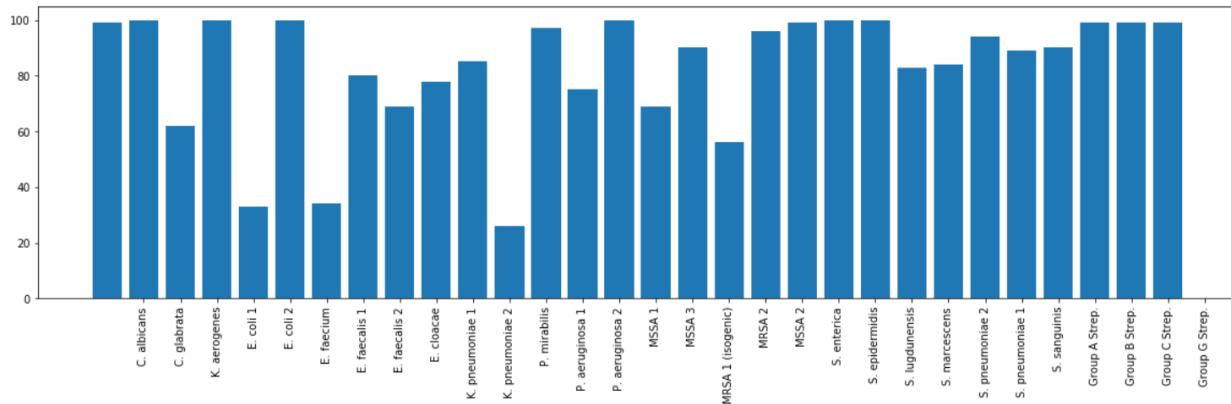


Fig. 8 The accuracies of bacteria

In fig 8, The accuracies for individual bacteria shown in the form of bar plot were the 10 class it predicts with 100% accuracy and 5 class with less than 60% accuracy. The overall accuracy using **1 D CNN is 81%**.

## VI. Conclusion

Due to lack of facilities of experimental owing to covid 19 situation, dataset is tested on machine learning algorithms on open-source dataset available from Stanford Medical Hospital and we achieve of 75% accuracy in it. Same Dataset is tested on 1D Resnet CNN architecture and the accuracy is 81%. Predicting many groups of bacteria, a group represents all the bacterial which can be treated with similar antibiotics. The same technique can be used for other cases to predict the classes and extract spatial features from dataset. From the results it is clear that the Deep Learning modules have more ability extract more spatial features than the Machine learning algorithms.

## REFERENCES

- [1] Karpathy, A & Fei-Fei, L. In Proceedings of the IEEE conference on computer vision and pattern recognition, 3218-3137(cv foundation.org, 2015).
- [2] Wang, L., Ouyang, W., Wang, X & Lu, H. In proceedings of the IEEE international conference on computer vision, 3119-3127 (cv-foundation.org,2015).
- [3] He, k., Zhang, X., Ren, S., & Sun, J. (2016). Deep Residual Learning for Image Recognition. 2016 IEE Conference on Computer Vision and PatterenRecognitin (CVPR).
- [4] Girshick, R., Donahue, J., Darrell, T. & Malik, J. In proceedings of the IEEE conference on computer vision and pattern recognition, 590-587 (cvfoundation.org, 2014).
- [5] Gallant, S.I. (1990). Perceptron-based learning algorithms. IEEE Transactions on Neural Networks.
- [6] Patel, S.V., Jokhakar, V.N. (2016). A random forest-based machine learning 2016 IEEE.
- [7] Navada, A., Ansari, A. N., Patil, S., & Sonkamble, B. A. (2011). Overview of use of decision tree algorithms in machine learning. 2011 IEEE control and system graduate Research Colloquim.
- [8] Kaming He, Xiaangyu Zhang, S Haoqing Ren & Jian Sun. "Deep Residual Learning for image recognition" 2016.
- [9] Dong, C., Loy, C.C., He, K. & Tang, X. In Computer Vision – ECCV 2014,184–199 (Springer International Publishing, 2014).



- [10] Lotfollahi, M., Berisha, S., Daeinejad, D. & Mayerich, D. Digital staining of High-Definition Fourier transform infrared (FT-IR) images using deep learning. *Appl. Spectroscopy*. 73, 556–564 (2019).
- [11] Berisha, S. et al. Deep learning for FTIR histology: leveraging spatial and spectral features with convolutional neural networks. *Analyst* 144, 1642–1653 (2019).
- [12] Berisha, S. et al. Deep learning for FTIR histology: leveraging spatial and spectral features with convolutional neural networks. *Analyst* 144, 1642–1653 (2019).
- [13] Kampe, B., Kloß, S., Bocklitz, T., Rösch, P. & Popp, J. Recursive feature elimination in Raman spectra with support vector machines. *Front. Optoelectronic*. 10, 273–279 (2017).
- [14] American Thoracic Society. & Infectious Diseases Society of America. Guidelines for the management of adults with hospital-acquired, ventilator associated, and healthcare-associated pneumonia. *Am. J. Respir. Crit. Care Med*. 171, 388–416 (2005).
- [15] Fleming-Dutra, K. E. et al. Prevalence of inappropriate antibiotic prescriptions among US ambulatory care visits, 2010-2011. *JAMA* 315, 1864–1873 (2016).